Forest Ecology and Management 496 (2021) 119386

Contents lists available at ScienceDirect

Forest Ecology and Management

journal homepage: www.elsevier.com/locate/foreco

Relating pre-fire canopy species, fire season, and proximity to surface waters to burn severity of boreal wildfires in Alberta, Canada

Prabha Amali Rupasinghe *, Patricia Chow-Fraser

McMaster University, Department of Biology, 1280 Main Street West, Hamilton, Ontario L8S 4K1, Canada

ARTICLE INFO

Keywords:
Boreal forests
Remote sensing
Wildfire
Canopy species mapping
Landsat

ABSTRACT

Increased global temperature, drought, and extreme weather have increased the frequency and intensity of wildfires in Canadian Boreal forests. We examined how burn severity was related to canopy species composition and proximity to water in six large boreal forest stands across northern Alberta (two in the Bistcho Lake region, three in Wood Buffalo National Park, and one in the Richardson backcountry) and a smaller stand close to the town of Slave Lake (204–5217 km^2). We used Landsat 5, 7, and 8 satellite images that included two phenological stages (spring, summer, or fall), followed by Support Vector Machines (SVM) classification to map the distribution of pre-fire canopy species. To quantify the burn severity of each fire, we used the Landsat images to calculate the differenced Normalized Burn Ratio (dNBR); we then combined dNBR for all affected areas to develop the Standardised Burn Impact Score (SBIS), that quantifies the average impact of each fire based on the size of the burned area and mean burn severity per pixel. In general, pre-fire dominance of coniferous species (jack pine and spruce) led to higher SBIS values while pre-fire dominance of broad-leaved species (aspen, birch, and poplar) led to lower values. Mean burn severity and SBIS values increased when fire events occurred at a distance of 1 km or greater from surface waters (e.g. lakes, rivers, and streams). We further analyzed the influence of fire season on burn duration and the proportion of canopy species being burned in each season. We found that fires that were ignited in spring lasted longer and burned more deciduous stands compared to fires that were ignited in summer. By integrating burn impact over very large temporal and spatial scales, we have confirmed the general influence of pre-fire canopy species on burn severity, and the ameliorating effect of surface waters on fire behavior at the landscape level.

1. Introduction

Boreal forests occur in northern circumpolar regions, where freezing temperatures are experienced for 6 to 8 months of the year (Mery et al., 2010). This biome encompasses ~30% of the global forested area and occurs in the northernmost regions of Canada, Russia, and the United States (Gauthier et al., 2015). They contain more surface freshwater than any other biome in the world (Mery et al., 2010) and store approximately 66% of the world's carbon in the soil, peat, and permafrost deposits and therefore, play a major role in global carbon cycling (Kasischke et al., 1995; Pan et al., 2011). They are also involved in global climate regulation through energy and water exchange (Steffen et al., 2015). Moreover, boreal forests provide great societal value by supporting fishing, hunting, leisure or spiritual pursuits, and economic opportunities to many rural communities as well as indigenous people throughout the world (Gauthier et al., 2015).

Boreal forests usually have low plant diversity with dominant gymnosperms such as white and black spruce (*Picea glauca* and *Picea mariana* respectively), jack pine (*Pinus banksiana*), balsam and douglas fir (*Abies balsamea* and *Pseudotsuga menzesii* respectively), and tamarack (*Larix laricina*) and varying proportions of angiosperms such as trembling aspen (*Populus tremuloides*), balsam poplar (*Populus balsamifera*), and white birch (*Betula papyrifera*) (Alberta Forest service, 1985; Mery et al., 2010; Shorohova et al., 2011). The canopy species are capable of reaching a minimum height of 5 m with a canopy cover of 10% (Gauthier et al., 2015). These forests are adapted to short, hot growing seasons, and long winters with extreme weather conditions (Matsuura, 2010). Furthermore, these forests are characterized by various disturbances including wildfire, insect infestations, and windthrow hazards, which are essential processes that maintain the structure and diversity of boreal forests (Gauthier et al., 2015).

Wildfire is considered the most widespread disturbance in boreal

* Corresponding author at: McMaster University, Department of Biology, Life Sciences Building, Room 206, 1280 Main St. West, Hamilton, ON L8S 4K1, Canada.
E-mail addresses: rupasinp@mcmaster.ca (P.A. Rupasinghe), chowfras@mcmaster.ca (P. Chow-Fraser).

https://doi.org/10.1016/j.foreco.2021.119386
Received 24 January 2021; Received in revised form 13 May 2021; Accepted 19 May 2021

forests that shape their structure, composition, and function, as well as influence rates and processes of ecological succession and encroachment (Lentile et al., 2006). Major factors that affect fire activity include availability and type of fuel, ignition agents, topography, human activities, and climate conditions (Johnson et al., 2001; Schoennagel et al., 2004). Flannigan et al. (2009) suggested that climate change can increase the area burned, the length of the fire season, the intensity as well as the severity of the fire; they predicted that the amount of burned area in Canada may increase by 74–118% by the end of the century. Given the importance of boreal forests, there is an urgent need to understand how specific factors contribute to the frequency and severity of wildfires and to monitor how boreal forests are responding to adverse effects of climate change (Chu & Guo, 2014).

Between 2004 and 2014, early-season fires in western Canada were more common compared to fires in summer and early fall, with a higher number of fire events and larger areas being burned (Bourgeau-Chavez et al., 2020). During spring, however, fires consumed less fuel and were less severe, burning less deeply and leaving unburned patches within the burn scar because fuel is still moist (Bourgeau-Chavez et al., 2020; Knapp et al., 2007, 2005). Despite this, early-season fires may have negative effects on forest regrowth, because these fires occur at the time when the plant growth rate is at its highest (Knapp et al., 2007). Therefore, understanding how fire seasonality influences different canopy species can help elucidate how fire regimes in Alberta will respond to climate change.

Severity and impact of wildfire in remote locations are also determined by a number of pre-fire conditions such as the distribution of pre-fire canopy species, local topography, fire weather, and fuel load and structure (Boucher et al., 2016; Krawchuk et al., 2016; Lydersen et al., 2017; Whitman et al., 2018). These factors are challenging to study because they require examination of multiple fire events occurring over large temporal and spatial scales that preclude the use of field studies. Even if logistical challenges can be overcome, severe fires can completely remove all traces of vegetation present before the fire. Therefore, remote sensing provides the best and most cost-effective means to understand fire behavior and pre-fire conditions over larger spatial scales (Akther and Hassan, 2011; Hall et al., 2008; Whitman et al., 2020, 2018).

Remote sensing images collected from satellites are widely used to study wildfires in North America because images can be acquired repeatedly over very large areas to permit long-term changes over large spatial scales (Barrett et al., 2011; Hall et al., 2008; Murphy et al., 2008; Whitman et al., 2020, 2018). Landsat, Moderate Resolution Imaging Spectrometer (MODIS), and Advanced Very High Resolution Radiometer (AVHRR) are some of the commonly used satellite sensors in remote sensing-based wildfire analysis and are especially useful in studying large wilderness areas (French et al., 2008; 1995; Kasischke and French, 1995; Moreno Ruiz et al., 2012; Potapov et al., 2008; Schroeder et al., 2011; Wulder et al., 2009). Landsat data, available since 1972, are the most popular because they offer a greater spectral and radiometric resolution, have global coverage, and are available at no cost (Chu and Guo, 2014; Whitman et al., 2020). Airborne data on the other hand provide high resolution images for a variety of purposes such as fire propagation modeling (Ononye et al., 2007). Airborne Light Detection and Ranging (LiDAR) are also commonly used to study wildfires and are useful in estimating fine-scale variability in forest structure, terrain, elevation, fire fuels as well as the post-fire recovery of vertical forest structure (Alonzo et al., 2017; Bolton et al., 2015; Karna et al., 2019). Spaceborne Synthetic Aperture Radar (SAR) is also being used for various fire studies such as post-fire regrowth and aboveground biomass, and soil moisture analysis (Kasischke et al., 2011; Lucas et al., 2012)

Burned vegetation has distinctively different reflectance signatures when compared with healthy vegetation. A drastic decrease of visible-to-near-infrared reflectance and an increase in short and middle infrared reflectance is observed in burned vegetation (Lentile et al., 2006; Miller and Thode, 2007). These shifts in reflectance signatures help to visualize burned areas in remotely sensed images and are the basis for many different methods such as remote sensing-based indices, hotspot analysis, thermal anomaly detection, change detection, and different modeling approaches (Chu and Guo, 2014; George et al., 2006; Kelhä et al., 2003; Remmel and Perera, 2001). Among these methods, spectral indices have been most commonly used, mainly due to ease of use. Differenced Normalized Burn Ratio (dNBR) (Key and Benson, 2005), Relativized dNBR (RdNBR) (Miller and Thode, 2007), and Relativized Burn Ratio (RBR) (Parks et al., 2014) are some of the common indices used to map burn severity. Besides mapping burn severity, remote sensing has also been used to map post-fire changes in landcover and vegetation recovery processes following fire events (Chu et al., 2016; Chu and Guo, 2014; Fernández-García et al., 2018; Hammill and Bradstock, 2006; Kokaly et al., 2007; Lentile et al., 2006; Leon et al., 2012; Miller and Yool, 2002).

Wildfires in boreal forests of northern Alberta have been large and frequent in recent decades (Stralberg et al., 2018), and a warming climate has been implicated as an important driver (Flannigan et al., 2009). Other variables such as the pre-fire composition of canopy species and proximity to surface waters (e.g. rivers, streams, and lakes) may influence burn severity at the stand level that could be important for managing wildlife habitat and for understanding fire behavior. Given that fire suppression generally resulted in a decrease in wildfire activity between 1980 and 2010 in Alberta's boreal forests (Robinne et al. 2016), studies should differentiate between wildfires that occur in remote, unmanaged areas and those that occur near human settlements that experience fire suppression and management.

The primary objective of this study was to use remote sensing to quantify the effects of pre-fire canopy species composition, duration and timing of fires, and proximity of surface waters on burn severity of multiple fire events occurring in boreal forests of northern Alberta. To minimize the variation in pre-fire conditions, we included fire events that occurred over an 11-y period between 2004 and 2015. To ensure our results have wide applicability, we chose four major areas in northern Alberta that experience a range of human disturbances from a minimal disturbance in a large national park to a forest stand located near a small town. To allow comparison of wildfire activity for each fire event, we created an index, the Standardized Burn Index Score (SBIS) that quantifies the average impact of each fire based on the size of the burned area and the mean burn severity per pixel. Overall, our goal was to provide a simple, cost-effective technique to quantify burn impact and fire behavior to investigate changes in fire regimes over large spatial and temporal scales.

2. Methods

2.1. Study sites

Our largest site is Wood Buffalo National Park (WB), Canada's largest National Park, and also one of the largest in the world (Lat 58.943 Lon −112.788; Fig. 1; Parks Canada 2020). The Park covers 44, 807 km^2 area in total and is characterized by large, undisturbed grass and sedge meadows, wetlands and prairie, and forests (UNESCO World Heritage Center, 2020). This park is very remote and is subject to the least anthropogenic stress, except for flow regulation, water withdrawal, industrial discharge, and effects of climate change, which originate from outside the park (UNESCO World Heritage Center, 2020). The Richardson (RC) Wildland Provincial Park is located 150 km southeast of WB National Park (Lat 57.999 Lon −111.141; Fig. 1), and is part of the largest sand dune complex in Canada, with paleo-parabolic dunes and riparian areas along the Athabasca River, and forests (Alberta Parks 2018). Bistcho Lake (BL) is located in northwestern Alberta (Lat 59.672, Lon −119.143; Fig. 1), and is characterized by wetlands, including *Sphagnum* peat bogs, channel fens, and large tracts of mixed wood forests (Alberta Wilderness Association, 2021). Other than wildfires, this area

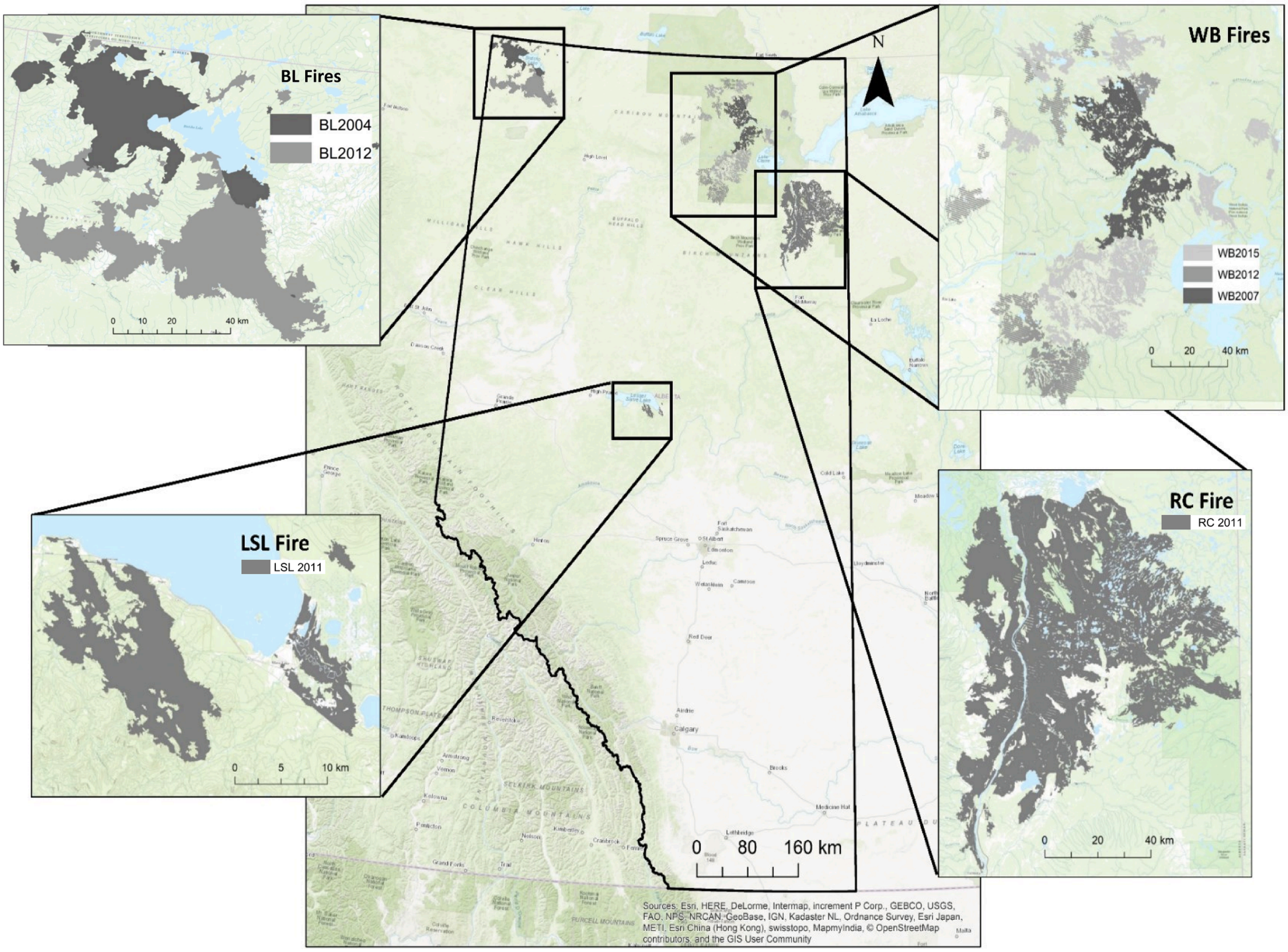

Fig. 1. Locations of fire events in four regions of Alberta's boreal forests used in this study (Base map: ESRI topographic maps).

has been disturbed by clear-cut logging and extensive petroleum and natural gas exploration for many years. Whereas only 22% of the Richardson area is disturbed by human activities, 61% of the Bitscho Lake area is anthropogenically disturbed with linear features (Canadian Parks and Wilderness Society Northern Alberta, 2016). The last study site is the Lesser Slave Lake region (LSL), located in the central part of Alberta, about 250 km northwest of the city of Edmonton (1.43 million as of 2019). The LSL fire occurred close to the Town of Slave Lake, near oil, gas, and forestry operations. In addition to the forest fire, 56 properties in the outskirts and one-third of the town were destroyed by this fire (Botey and Kulig, 2014).

All fire events occurred after 2004, during the spring to fall months, and the burned areas varied from 204 to 5217 km^2. In total, we studied seven fire years within our four study sites. There were two fire-years in BL (2004 and 2012) and three in WB (2007, 2012, and 2015 in WB) whereas both RC and LSL were single fire events that occurred in 2011 (Table 1).

2.2. Image data

We used Landsat 5, 7, and 8 multispectral images for burn-severity calculation and species mapping. Landsat is owned by the United States Geological Survey (USGS) and the National Aeronautics and Space Administration (NASA) and is the longest earth observing satellite series. Landsat 5 operated from March 1984 to January 2013. For this study, we used six bands of Landsat 5 Thematic Mapper (TM): blue (0.45–0.52 μm), green (0.52–0.60 μm), red (0.63–0.69 μm), two Near-Infrared (NIR) bands (0.76–0.90 and 0.76–0.90 μm), and Mid-Infrared (2.08–2.35 μm) (USGS, 2016a). Landsat 7 was launched in April 1999 and is still functioning. We used seven bands of Landsat 7: blue (0.45–0.52 μm), green (0.52–0.60 μm), red (0.63–0.69 μm), two NIR (0.77–0.90 and 1.55–1.75 μm), and Mid-Infrared (2.08–2.35 μm) (USGS, 2016b). Landsat 8 is the newest satellite of the series which was launched in February 2013. We used seven bands of Landsat 8 Operations Land Imager (OLI): coastal aerosols (0.43–0.45 μm), blue (0.45–0.51 μm), green (0.53–0.59 μm), red (0.64–0.67 μm), NIR (0.85–0.88 μm), and two Shortwave Infrared (SWIR) bands (1.57–1.65 and 2.11–2.29 μm). All images have a 30-m spatial resolution.

We downloaded cloud-free images before and after fire events, or those with minimum cloud cover from Earth Explorer to map burn severity (Table 2). For species mapping, we downloaded additional images either acquired in spring or fall (further explained in Section 2.5). For the Landsat 7 images, we used an additional image acquired as close as possible in date to the first image to fill data gaps caused by a sensor-borne error. We used ENVI 5.5 (Harris Geospatial Solutions) to preprocess and process reflectance values in our images. We performed radiometric correction and atmospheric correction (ENVI FLAASH), rescaled reflectance from 0 to 1, and masked clouds as well as shadows cast by clouds, and any thick haze in images. We manually created Regions of Interests (ROIs) for these features in ENVI and used the build mask tool to produce the masks.

Table 1
Start and end dates, burn duration, season, and area affected by different fire events in this study (Natural Resources Canada, 2017; U.S. Fire Administration, 2005).

Fire event	Start date	End date	Burn duration (d)	Season	Area affected (km^2)
WB 2007	2007–05-29	2007–07-13	45	Spring-summer	665.16
	2007–05-29	2007–08-01	64	Spring-summer	790.05
WB 2012	2012–05-26	2012–09-28	125	Spring-summer	874.91
	2012–06-08	2012–08-08	61	Spring-summer	245.28
	2012–07-09	2012–07-28	19	Summer	31.52
	2012–07-10	2012–07-16	6	Summer	211.97
	2012–07-10	2012–08-22	43	Summer	24.38
	2012–07-13	2012–08-22	40	Summer	90.86
WB 2015	2015–05-28	2015–10-01	126	Spring-Fall	1315.59
	2015–06-05	2015–07-05	30	Spring-summer	209.58
	2015–06-06	2015–07-12	36	Spring-summer	207.93
	2015–06-18	2015–08-11	54	Spring-summer	229.47
	2015–06-24	2015–09-12	80	Spring-summer	140.84
	2015–06-26	2015–09-12	78	Spring-summer	223.97
LSL 2011	2011–05-04	2011–05-17	13	Spring	203.63
RC 2011	2011–05-14	2011–07-06	53	Spring-summer	5217.36
BL 2004	2004–07-12	2004–09-26	76	Summer	989.25
	2004–07-15	2004–08-10	26	Summer	126.13
	2004–07-22	2004–08-16	25	Summer	15.60
BL2012	2012–06-22	2012–10-07	107	Spring-fall	1886.26
	2012–08-12	2012–09-23	42	Summer	119.61

Table 2
Year and location of fires in the study, and satellite images used in associated burn severity analyses. L5, L7, and L8 refer to Landsat 5, Landsat 7, and Landsat 8, respectively.

Year of fire	Location of fire	Image used before the fire		Image used after the fire	
		Date acquired	Sensor	Date acquired	Sensor
2011	LSL	2010/06/19	L7	2011/08/09	L7
		2010/07/21	L7	2011/08/25	L7
2011	RC	2010/07/23	L7	2011/09/04	L5
		2010/08/24	L7		
2007	WB	2006/09/04	L5	2008/06/21	L5
2012	WB	2011/09/10	L7	2013/08/06	L8
2015	WB	2014/09/10	L8	2015/09/29	L8
2004	BL	2003/08/30	L5	2005/08/12	L5
		2003/09/01	L5		
2012	BL	2011/09/14	L5	2013/07/10	L8
				2013/09/03	L8

2.3. Mapping burn severity

We calculated the dNBR (equations (1) and (2)) to map burn severity (Key and Benson, 2005) using the preprocessed Landsat images collected before and after the fire event (Table 1).

$$NBR = \frac{(NIR - SWIR)}{(NIR + SWIR)} \tag{1}$$

$$dNBR = NBR_{prefire} - NBR_{postfire} \tag{2}$$

where NIR and SWIR are the corresponding image bands and the $NBR_{prefire}$ and $NBR_{postfire}$ are the corresponding NBR calculated for images acquired before and after the fire event. The dNBR values were imported into ArcMap 10.4.1 and these were classified into burn-severity classes according to guidelines in Table 3. We used the shapefiles of the burn footprint available from the Canadian National Wildfire Database (CNFDB) (Natural Resources Canada, 2017) to determine the size and the borders of the burned area for each fire event.

2.4. Mapping canopy species distribution

2.4.1. Ground reference data

To map the distribution of canopy species before the fire event, we used ground reference data from Phase 3 of the forest inventory monochrome maps created by Alberta Township Systems (ATS) (Alberta Government, 2019). In total, three forest inventories were conducted in Alberta; Phase 1 included most of the publicly owned forested lands, while Phase 2 covered lands with commercial timber commitments. Phase 3 is the most recent inventory that was initiated in 1970 and was completed in 1984. It covered both forests on publicly owned lands as well as areas of active timber harvesting (Alberta Forest service, 1985) and included greater detail on canopy species. Training data for these maps were derived from aerial photographs and were combined with field data that documented stand volumes and growth estimations. Photointerpretation was conducted manually (minimum stand size of 2 ha) and included species composition (based on ground surveys), crown density, height, date of stand origin, site index class, and coniferous commercialism class (Alberta Forest service, 1985).

We first digitized the species locations from the monochrome maps using ArcGIS. For this step, we used locations that had been affected by the fire as well as the unaffected areas between 1985 and 2017. When digitizing, we avoided using mixed-species locations of the Phase 3 ATS maps; instead, we only used locations corresponding to a single species to ensure the usage of pure signals as training data. The forest inventory data did not cover the northernmost part of Alberta entirely, therefore we only had ground reference partially for WB and BL burned areas. In that case, we used more species locations from neighboring regions as ground references and used them in image classification and validation. We used 70% of the training data for image classification and reserved the remaining 30% for testing the accuracy (i.e., validation data).

2.4.2. Image classification

The Landsat images collected in two seasons, either spring and

Table 3
Burn Severity categories according to U.S. Geological Survey FireMon program (Key and Benson, 2005).

dNBR value	Burn Severity Category
< −0.25	High post-fire regrowth
−0.25 to −0.1	Low post-fire regrowth
−0.1 to 0.1	Unburned
0.1 to 0.22	Low burn severity
0.22 to 0.44	Low-moderate burn severity
0.44 to 0.66	Moderate-high burn severity
>0.66	High burn severity

Table 4
Satellite images used for tree species mapping before fires at LSL 2011, RC 2011, WB 2007, 2012, and 2015, and BL 2004 and 2012.

Fire	Focal year	First season image		Second season image	
		Date acquired	Sensor	Date acquired	Sensor
LSL	1986	1986/06/02	L5	1986/08/28	L5
	2010	2010/06/20	L5	2010/09/24	L5
RC	1985	1985/07/03	L5	1985/08/18 &	L5
				1985/09/28	L5
	2010	2010/07/22 &	L5	2010/10/03	L5
		2010/07/24	L5		
WB	1985	1985/07/17 &	L5	1985/09/10	L5
		1985/07/31	L5		
	1997	1997/06/23	L5	1997/08/26	L5
	1998	1998/06/10	L5	1998/08/26	L5
BL	1985	1985/06/02	L5	1985/08/21	L5
	2002	2002/06/09	L7	2002/09/13	L7
	2006	2006/06/12	L5	2006/08/31	L5
	2008	2008/05/16	L5	2008/07/03	L5

summer, fall and summer, or spring and fall, were stacked together as a layer stack prior to image classification (see Table 4). We followed the methods developed by Liu et al. (2002) and used the Support Vector Machines (SVM) in ENVI 5.5 to classify images. Using this procedure, we produced classified images beginning in 1985 until each fire event in our study. We combined the dominant deciduous species (aspen, birch, and poplar) into one class because our classification was unable to accurately discriminate among these species. We were also unable to discriminate between white and black spruce and combined them into a single class to improve classification accuracy. Our final classification scheme included three taxon classes and two non-vegetated classes: deciduous (aspen, birch, or poplar), spruce (black or white), jack pine, water, and unvegetated area. We obtained the maximum possible classification accuracy for 1985/6 (over 70% for the majority of the cases) by carefully comparing every ROI digitized from the ATS maps with the Landsat images and removing locations that seem to be unvegetated or within clouds, cloud shades, or haze. We then used the same ROIs from the 1985/6 classification to classify the images collected before the fire event (Table 4). Here we carefully checked the ROIs again for every pre-fire year in the time series and excluded the ROIs that were located within clouds, shadows of clouds, clear cuts, or areas that appeared to have been disturbed. We used multiple pre-fire years following the initial ground truth data collection (Table 4) to update the ground truth until the most recent pre-fire maps to eliminate any ROIs on clear cuts or canopy damage that may have re-grown with different species. Given that our study sites had minimal human disturbance, we assumed that the forest canopy species composition in the ground reference locations did not change between 1985/1986 until the most recent pre-fire year unless there was a visible change. After the image classification, we applied a 3 by 3 majority filter to smooth out the classified images.

2.5. Standardized burn impact score (SBIS)

We developed SBIS to characterize the impact of each fire event using the equation below.

$$SBIS = Average\ dNBR\ per\ square\ km \times Total\ area\ burned\ (km^2) \quad (3)$$

For each fire event, we extracted dNBR values for all the pixels within the burned area and calculated the average dNBR values. Then we calculated the average dNBR per square kilometer (as Landsat is 30 m spatial resolution) to be used in equation (3). We calculated the total burned area using the burned area shapefiles downloaded from Natural Resources Canada (2017). We calculated this score for each of the 21 fire events within the study locations.

2.6. Pre-fire species composition data analysis

Following the image classification, we conducted further analysis in ArcMap 10.4.1. We clipped the classified maps with the fire footprint (Natural Resources Canada, 2017) and intersected it with the reclassified dNBR maps to combine pre-fire canopy species distribution with the burn severity levels (Section 2.3). Then we calculated the area and the percent area of each land cover type within each burn severity class, and this was performed separately for each fire event. We used these area and percent area values for further statistical analysis.

We also extracted the species composition within 21 smaller fire events regardless of the burn severity category and analyzed the relationship between species composition and average dNBR and SBIS using regression analysis. We conducted all analyses with Microsoft (MS) Excel and JMP 15 software.

2.7. Impact of seasonality and land cover on burn severity

We used the fire information from CNFDB to determine the timing of fire events and extracted the corresponding percentage cover of deciduous, coniferous, and unvegetated areas (discussed under Section 2.4). We then related the seasonality of fire events (i.e. occurring in spring (SP; May-June), summer (SM; July-August), and fall (FL-September-October) to pre-fire canopy species for each fire event.

2.8. Burn severity and impact in relation to proximity to surface waters

We extracted the surface waters from classified maps (Section 2.4.2) and modified these visually to minimize the classification errors using ArcGIS to investigate the effect of surface waters such as rivers, lakes, and ponds on the burn severity. We created multiple ring buffers around surface waters at 50, 100, 150, 200, 250, 500, 1000, 1500, and 2000 m intervals. Then we extracted the dNBR values within each of the buffers for 21 smaller fire events. We calculated average dNBR and SBIS for all buffers and fire events separately and regressed these values against proximity to surface waters.

3. Results

3.1. Burn severity and impact

Burn severity and the areal extent of the seven fire years within the four study sites varied greatly (Fig. 2). The RC fire in 2011 was the largest, burning a total area of 4942.0 km^2 according to our assessment using dNBR of the affected area (5217 km^2) recorded by the CNFDB. This was followed by the WB fire in 2015, which burned a total of 2194.03 km^2; out of 2327.39 km^2 area recorded by the CNFDB was burned (Fig. 2 a and b). Although the LSL fire was the smallest, with only 154.01 km^2 burned out of the recorded area of 203.63 km^2 (Fig. 2b), it had a disproportionately large area with high burn severity (45.24%; Fig. 2c). The BL 2004 fire had the second-largest percentage area of high burn severity, given the total burned area reported in the CNFDB (39.51%; Fig. 2c). The WB 2007 fire burned with the lowest severity, with only 0.32% of the total area associated with high burn severity while 54.58% was associated with low burn severity (Fig. 2c). Overall, most locations experienced moderate-high and high severity burns except for the WB 2007 and 2012 fires, which had low and moderate-low severity fires in the majority of the burned area. When the total affected area recorded by the CNFDB is considered, LSL and WB 2007 site-events had more unburned than burned areas according to our approach of burn mapping using dNBR. When average dNBR for the site events are considered, WB 2007 fire had the lowest dNBR value (average of 0.073; Table 5), followed by the LSL fire (0.156). By contrast, the highest average dNBR was for the BL 2004 fire (average of 0.643). However, when the total affected area is combined with the dNBR through SBIS, the least burn impact was on the LSL fire (35,496.03),

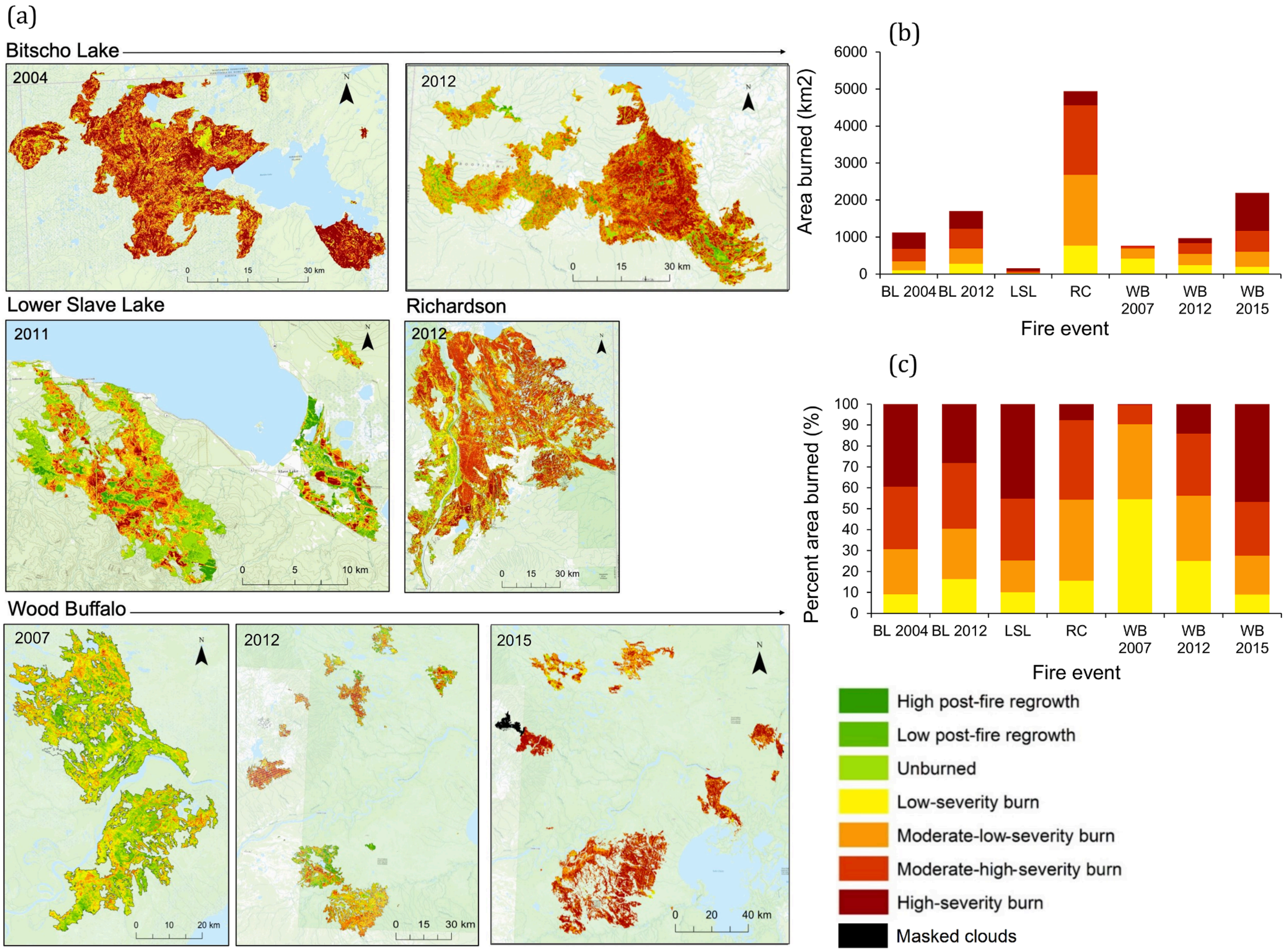

Fig. 2. Comparison of burn severity of the study sites (a) burn severity maps of fire events based on dNBR values (Note: fire perimeters shown in the maps are the existing boundaries from CNFDB and the light blue color areas of the base map within the burned areas are the unburned islands recorded by the CNFDB), (b) areas burned at different burn severity levels determined from dNBR, and (c) percent area burned at each burn severity level. (Base map: ESRI topographic base map). (For interpretation of the references to color in this figure legend, the reader is referred to the web version of this article.)

Table 5
Average dNBR and SBIS of fire events determined using the fire perimeters from CNFDB.

Site	Start date	End Date	Average dNBR	SBIS
WB 2007	2007–05-28	2007–07-13	0.076	56489.674
	2007–05-28	2007–08-01	0.069	60719.707
WB 2012	2012–05-26	2012–09-28	0.307	298543.927
	2012–06-08	2012–08-08	0.347	94534.736
	2012–07-09	2012–07-28	0.432	15133.823
	2012–07-10	2012–08-22	0.442	11965.194
	2012–07-10	2012–07-16	0.527	124048.955
	2012–07-13	2012–08-22	0.197	19921.593
WB 2015	2015–05-28	2015–10-01	0.661	965751.102
	2015–06-05	2015–07-05	0.789	183343.620
	2015–06-06	2015–07-12	0.406	93664.958
	2015–06-18	2015–08-11	0.647	164716.222
	2015–06-24	2015–09-12	0.676	105712.944
	2015–06-26	2015–09-12	0.443	112636.689
BL 2004	2004–07-12	2004–09-26	0.573	629835.516
	2004–07-15	2004–08-10	0.819	114730.527
	2004–07-22	2004–08-16	0.538	9325.333
BL 2012	2012–06-22	2012–10-07	0.435	912120.341
	2012–08-12	2012–09-23	0.195	25938.757
RC 2011	2011–05-14	2011–09-09	0.350	2029980.823
SL 2011	2011–05-14	2011–05-17	0.156	35496.026

followed by the WB 2007 fires (average of 58,604.69). The highest burn impact was for the RC fire (2,029,980.823) (Table 5).

3.2. Burn severity and pre-fire species distribution

We obtained greater than 75% accuracy for both overall and species level accuracy (Table 6). The use of two seasons' images improved mapping accuracy by about 20% over than when single images were used; however, since there were a limited number of cloud-free images

Table 6
Overall and canopy species mapping accuracy of time series species maps for initial data collection year and most recent pre-fire year landcover maps.

Fire	Focal year	All Classes		Canopy species	
		Overall accuracy (%)	Kappa	Overall accuracy (%)	Kappa
LSL	1986	82.13	0.75	79.38	0.67
	2010	80.92	0.74	80.44	0.61
RC	1985	92.65	0.88	91.66	0.72
	2010	88.20	0.80	85.21	0.73
WB	1985	90.09	0.87	83.75	0.66
	1998	82.47	0.76	77.22	0.59
BL	1985	88.89	0.76	89.81	0.67
	2002	79.53	0.68	84.60	0.55
	2008	77.75	0.64	78.02	0.60

over two seasons in the same year, we could not create the most recent pre-fire landcover maps for most of the fire events.

In all cases, coniferous species dominated the pre-fire canopy, occupying more than half of the area. RC was the largest burned area (5217.36 km^2), which had a pre-fire composition consisting of >80% jack pine (Figs. 3 and 4). Areas with low burn severity coincided with areas occupied by the deciduous taxa, accounting for <6% cover and pre-fire unvegetated areas (Figs. 3 and 4). By contrast, the pre-fire canopy in burned areas at WB during 2007, 2012, and 2015 were dominated by spruce (73%, 58%, and 57% respectively). The WB fires consisted of multiple fire events, two in 2007, seven in 2012, and six in 2015 (Table 1). The pre-fire species in the BL area was also dominated by spruce, which occupied 54% and 76% of the burned areas in 2004 and 2012, respectively (Figs. 3 and 4); the higher coniferous cover in the latter year may reflect the higher area burned in 2012 (2005 km^2) compared with that in 2004 (1130 km^2) (Fig. 2b). The smallest fire in this study occurred near Lesser Slave Lake (LSL), where spruce occupied 59% of the pre-fire canopy (Figs. 3 and 4).

In general, the burn severity categories appeared to be dependent on the pre-fire species distribution; in areas dominated by aspen, birch, or poplar, burn severity categories remained low or moderate-low, whereas in areas dominated either by spruce or jack pine, burn severity levels reached high or moderate-high categories (Fig. 4 and Table 7). We also pooled all sites to statistically test the relationship between burn severity and species distribution of the forest canopy. There was a significant negative relationship when burn severity was regressed against the percentage cover of deciduous taxa in the pre-fire forest stands ($R^2 = 0.30$, $p < 0.0001$). In contrast, we found a significant positive relationship when burn severity was regressed against the percentage cover of spruce in the pre-fire forest stands ($R^2 = 0.31$, $p < 0.001$) (Table 7).

We found a significant positive correlation between burn duration and total burned area ($r = 0.62$; $p = 0.003$). When average dNBR values were regressed against burn duration, percent cover of deciduous, and percent cover of coniferous species, we did not find any significant relationship (Fig. 5 a, b, and c, respectively). By contrast, we found a significant non-linear relationship between SBIS and burn duration, coniferous species, and the areal cover of deciduous species (Fig. 5 d, e, and f, respectively).

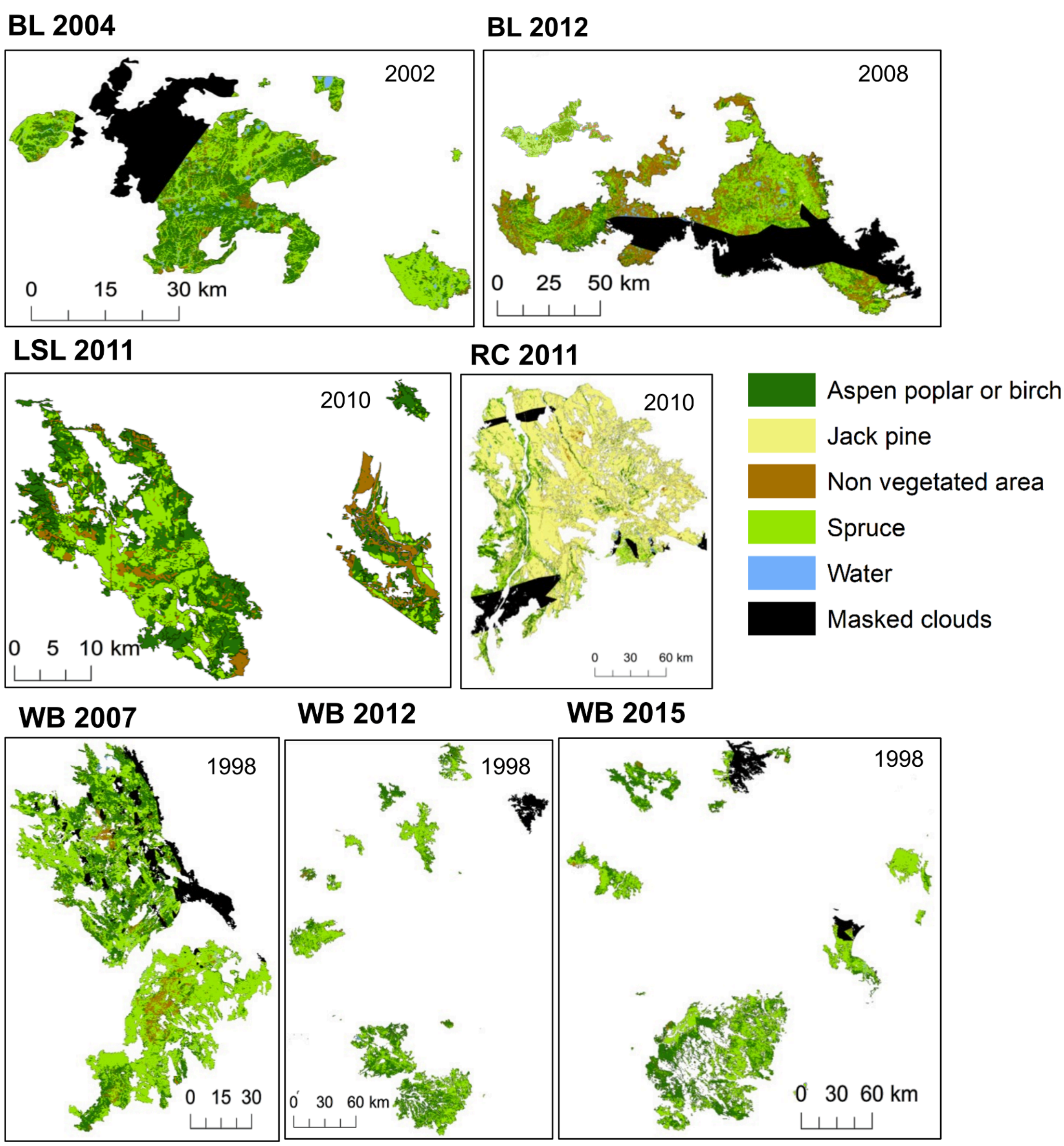

Fig. 3. Distribution of tree species within the fire footprints before fire events.

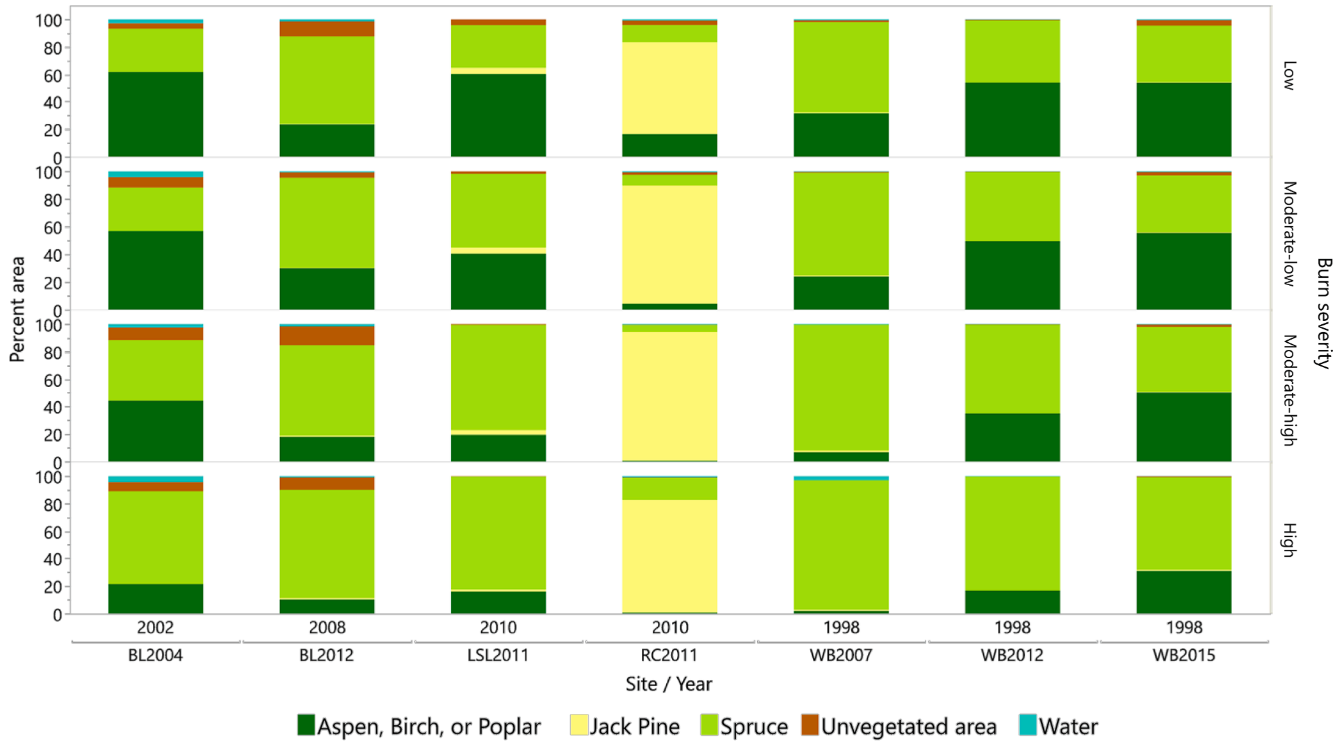

Fig. 4. Percentage landcover classes for four burn-severity categories based on most recent pre-fire land cover maps.

Table 7
Summary statistics for linear regression analyses relating percent total area burned to burn severity category for the four sites and when data from all fire years were pooled. Regression equations were determined separately for coniferous and deciduous species. (The significant values are indicated with *).

Location	Species	Regression coefficient	R-square	P-value
LSL	Spruce	16.014	0.93*	0.0001*
	Aspen, birch, or Poplar	−14.384	0.93*	<0.0001*
RC	Jack pine	6.192	0.78*	0.1146
	Aspen, birch, or Poplar	−5.102	0.78*	0.1196
WB	Spruce	7.694	0.29	0.0007*
	Aspen, birch, or Poplar	−6.066	0.21	0.0045*
BL	Spruce	8.521	0.33	0.0014*
	Aspen, birch, or Poplar	−8.841	0.39	0.0003*
All Sites	Spruce or Pine	+8.795	0.31	<0.0001*
	Aspen, birch, or Poplar	−7.913	0.30	<0.0001*

3.3. Impact of seasonality on burn severity

Based on the studied fire events, fires started during May and June lasted longer than those that started in July (one-way ANOVA; $p=<0.001$ and $p = 0.0028$ respectively); on the other hand, durations of fires that started in August were not significantly different from those that started in May, June, or July (Fig. 6a). Duration of fires that ended in May and July were statistically similar and significantly shorter than those in the latter months, with successively longer durations for each month from August to October (ANOVA; Tukey-Kramer post-hoc comparisons; $p=<0.001$ for all pairs, except $p = 0.002$ for October and September and $p = 0.013$ for August and July) (Fig. 6b).

For fires that started in May to July, a higher percentage cover of conifers was burned compared with those that started in August (Fig. 7a). By comparison, fires that started in August had a higher percentage of deciduous species burned compared with other months (Fig. 7a). Percentage unvegetated areas were generally low across the summer months, although values were slightly higher for fires that started in August. Fires that ended in May had the lowest percentage cover of coniferous trees and the highest cover of deciduous trees (Fig. 7b). Moreover, a higher unvegetated area was burned if the fire ended in May compared to those that ended later in the summer (Fig. 7b). A smaller percentage of coniferous cover burned if fires started and ended in spring compared with fires that lasted multiple seasons, or those that occurred during only the summer months (Fig. 7c). By comparison, a higher percentage of deciduous cover was burned in spring fires (Fig. 7c) and relatively more unvegetated areas were burned in fires that occurred during spring.

3.4. Burn severity and impact in relation to proximity to surface waters

We observed a strong logarithmic relationship between average dNBR and the distance from surface waters ($R^2 = 0.76$, Fig. 8a). dNBR increased sharply from 0 to 150 m, reaching a plateau at l km away from surface waters. When individual fire events were considered, we found significant relationships for 13 of the 21 fire events; regression analysis for six of the WB and two of the BL fire events, however, did not result in any significant relationship.

As we did not observe a change in dNBR after a distance of 1 km, we investigated the relationship between SBIS value and the effect of surface waters within a 1 km buffer only (Fig. 8b). We obtained a highly significant linear relationship ($R^2 = 0.9686$) between average SBIS for all fire events and their distance to surface waters (Fig. 7b). When individual fire events were considered, we obtained highly significant ($R^2 > 0.95$) relationships between SBIS and distance to surface waters for all 21 fires regardless of burn severity.

4. Discussion

Wildfires are the main stand-renewing disturbance in boreal forests

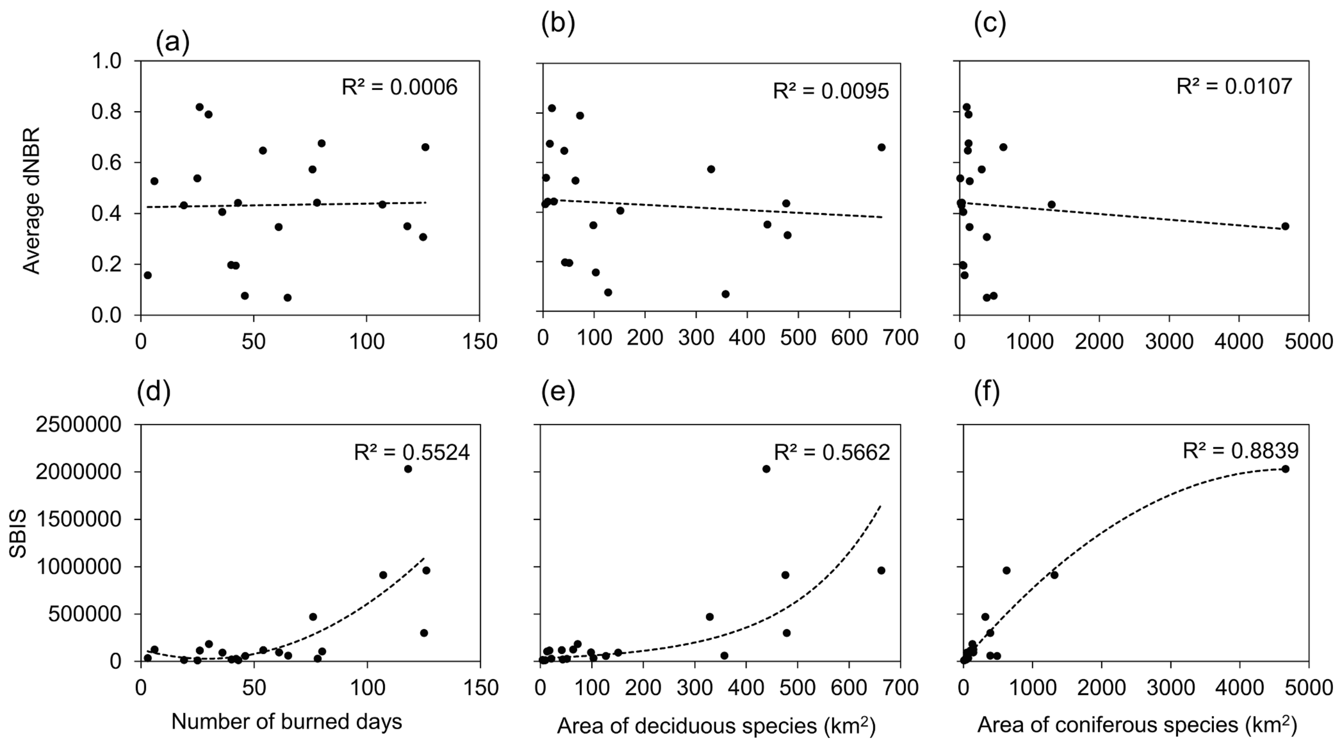

Fig. 5. Linear regression of burn severity (dNBR) against (a) burn duration, (b) percent area of deciduous species, and (c) percent area of coniferous species; non-linear regression of SBIS against (d) burn duration, (e) area of deciduous species, and (f) area of coniferous species.

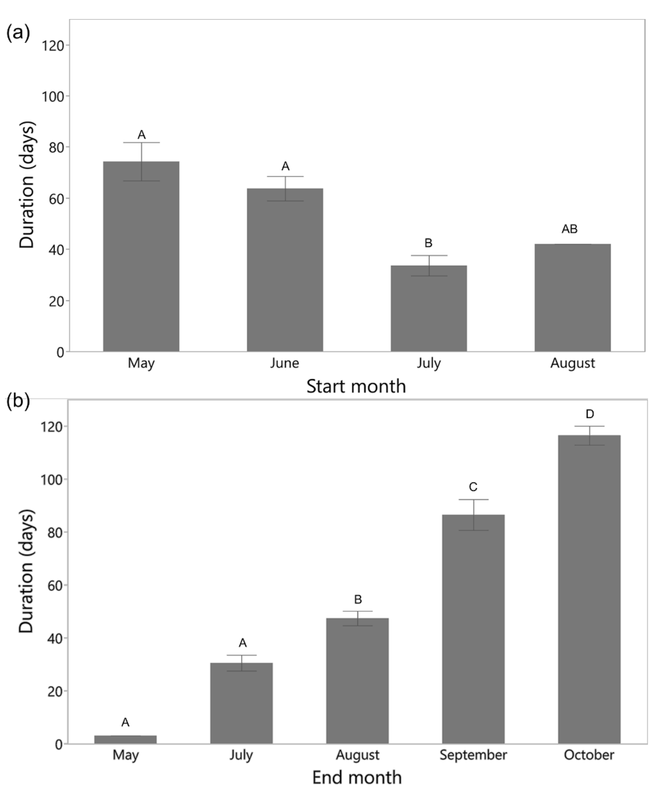

Fig. 6. Mean (±SE) burn duration associated with (a) month that fires started and (b) month that fires ended.

(Parisien et al., 2005). Fire regimes are variable over both space and time. To understand these dynamic systems, quantification of fire magnitude in terms of both burn severity and impact is essential.

Acquiring burn severity data is often challenging in remote regions of northern Alberta due to limited access and the high cost of surveying. This becomes even more challenging when investigating historical fire events since the affected areas have been in recovery for many years or even decades. Remote sensing can overcome these challenges and may be the only viable option in the Canadian boreal region (Boucher et al., 2016; Hall et al., 2008; San-Miguel et al., 2016; Soverel et al., 2010; Whitman et al., 2018).

In this study, we used dNBR, a widely used index of burn severity developed by Key and Benson (2005). This index was first developed in 1996 following a wildfire at Glacial National Park, the USA in 1994. The Composite Burn Index (CBI) was also developed to field validate the burn severity index (Key and Benson, 2005). Since then, dNBR has been widely investigated, used with various satellite sensors (eg: Landsat, AVIRIS, MODIS), and calibrated with field measurements (Chuvieco et al., 2006; Cocke et al., 2005; Keeley, 2009; Kokaly et al., 2007), making it the index of choice for mapping burn severity throughout North America (Hall et al., 2008; Loboda et al., 2007; San-Miguel et al., 2016; Soverel et al., 2010). Although we did not have ground reference data to assess the accuracy of burn severity determined through dNBR, we believe that the dNBR provided reliable results on burn severity as it had been widely used for burn severity assessment in Alberta (Peddle et al., 2007; Soverel et al., 2011; 2010; 2010; Whitman et al., 2020, 2018). Furthermore, the burn severity categories derived through dNBR corresponded well with the degree of vegetation changes in affected areas investigated using Normalized Difference Vegetation Index (NDVI) and Leaf Area Index (LAI) (Rupasinghe and Chow-Fraser, unpublished data) and therefore, we believe that the dNBR and the burn severity classes provided a reliable result (Soverel et al., 2010). In some cases, the burned areas detected through our methods differed somewhat from the fire scars recorded by CNFDB. This is due to the unavailability of cloud-free images immediately following the fire events, and in those cases, forest regrowth may have occurred between the end of the fire and the acquisition of the post-fire image.

Despite the high accuracy and widespread use of dNBR, the index only gave a measure of burn severity of an image pixel. Therefore, the

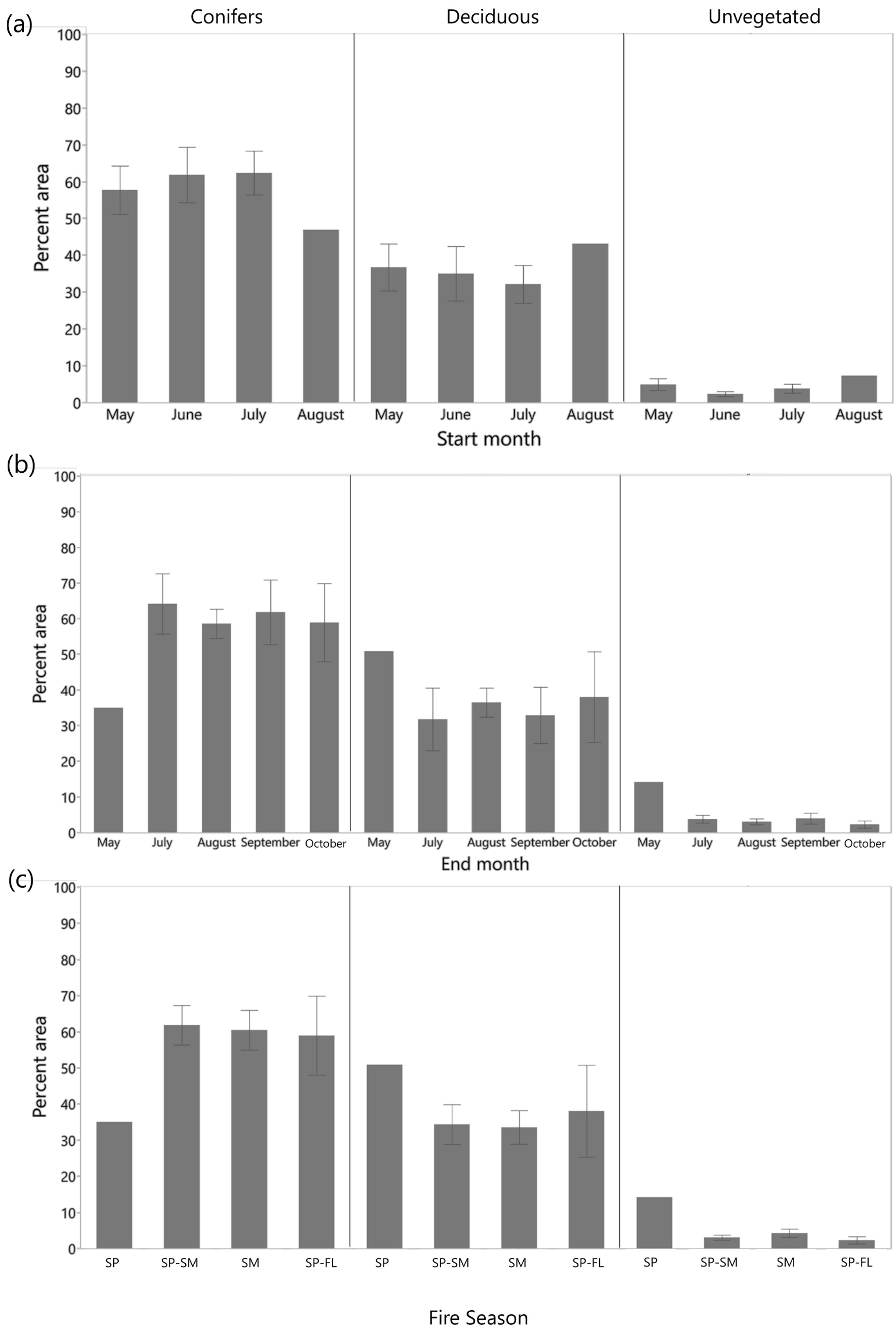

Fig. 7. Mean (±SE) percentage area burned for land cover types based on (a) month that fire started (b) month that fire ended, and (c) season(s) when fires occurred (SP = spring; SP-SM = spring to summer; SM = summer; SP-FL = spring to fall).

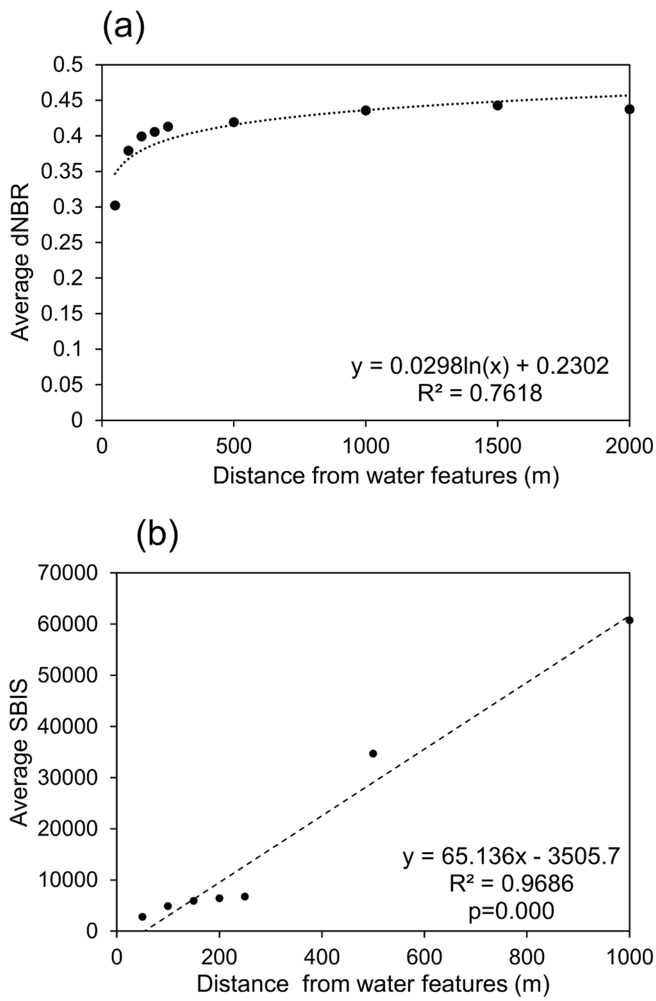

Fig. 8. Regression analysis of (a) dNBR and (b) SBIS of fire events against proximity to surface waters.

results are presented in a format of a map or graph. The impact of fire, however, depends on both fire severity and the area affected. By calculating the average dNBR value for all pixels in the burned area, we were able to integrate the impact of a particular fire event into a standardized score by accounting for both area affected and the burn severity. The SBIS, which is simple to calculate and use, could rank the severity of fire events, regardless of their size. We related SBIS values to pre-fire conditions to produce a generalized understanding of how the type of pre-fire canopy species contributed to burn severity. Moreover, since the SBIS accounts for the size of the area affected, it is a better option to use when comparing fires of approximately similar size.

The fire season in Alberta usually starts in early April and ends in October and most of the fires occur in the northern region (Tymstra et al., 2005). All the fire events we investigated occurred within this time frame. Based on our results, fires started early in the season tend to burn longer regardless of the burn severity. Generally, fire impact on deciduous species was greater early in spring and late in the fall, whereas the impact on conifers was greatest in mid-season. This may be because lack of leaves in spring and drier conditions towards late summer and early fall can facilitate the burning of deciduous stands. According to Knapp et al., (2007), early season fires raise concerns because the fires may inhibit the vegetation recovery due to peak plant growth occurring this season. Despite the fact that deciduous trees are naturally less prone to fire, half of our studied fires started in spring and extended into the summer and/or fall and burned a comparatively higher percentage cover of deciduous stands.

Majority of the fire events we investigated experienced moderate-high to high severity fires. The WB and RC fires, however, were exceptions, with moderate or low burn severity in most of the affected areas. The forests in the footprint of the WB 2007 and RC 2011 fires had experienced partial burns in the early 1950s and 1980s, respectively (Alberta wildfire, 2020). These earlier fires may have reduced fuel accumulation and prevented high burn intensity in the more recent fires. Furthermore, all WB 2007 fires started in early spring and this may have also contributed to low burn severity despite that the fires lasted longer. Similarly, the 2012 event in WB was not due to a single large fire but six smaller fire events with less severe burns, likely because the area had been surrounded by many historical fires and the meanders of the Peace river had acted as natural fire barriers. Although we did not investigate it, these anomalies may also have been due to site-to-site variation in weather conditions (precipitation and temperature).

It is also important to consider the influence of anthropogenic disturbances (e.g. oil explorations, human settlements) as well as fire management. Among the fire events studied within regions, WB was the least affected by anthropogenic activity, and this was followed by the RC fire. These two regions are in protected areas and have minimal to no impact from oil and gas exploration and human development. The BL area, however, is severely affected by both gas and oil exploration as well as logging, with a very high density of seismic lines. Of the four regions, the LSL fire was the most affected by anthropogenic activity and fire management. This fire event was the smallest, and in fact, about 25% of the affected area recorded by the CNFDB was not mapped as being burned by dNBR, although there was high burn severity, probably due to the higher amount of accumulated fuel in the forest. However, this fire occurred only for few days in spring and this may have resulted in a smaller burned area as well as faster recovery.

The LSL fire was anomalous to the other three regions, likely because of its proximity to the town of Slave Lake. Despite the high burn severity, if we considered both the area burned and mean severity together, the LSL fire exerted the least impact overall. According to Robinne et al., (2016), human activities are expected to reduce fire activity close to human settlements. Human involvement in fire suppression and management makes natural fire behavior more complex to understand and for which to predict future trajectories (Robinne et al., 2016; Thompson and Calkin, 2011).

In this study, we confirmed that the pre-fire composition of canopy species in forests had a significant effect on burn severity. Cumming (2001) also used Alberta Phase 3 inventory (Alberta Forest service, 1985) to investigate the relationship between the forest type and wildfire in northeastern Alberta. They used Volronoi polygonization as approximate digitization of the forest stand boundaries followed by statistical and modeling approaches. In our study, however, we used remote-sensing image classification followed by GIS-based analysis to achieve the same objective. The use of multitemporal images from the Landsat satellite alone with the automated image classification approaches considerably reduced the need for time-consuming digitizing as well as person-related errors. Furthermore, we were able to obtain a good level of accuracy for overall and target species mapping. Despite differences in methods used, Cumming (2001) reported similar results to ours, where deciduous stands burnt at a lower rate while black spruce stands burned at the highest rate. Moreover, repeating our methods with higher resolution images may further improve the mapping accuracy.

Cumming, (2001) has listed the boreal canopy species in decreasing order of fire susceptibility as black spruce, pine, white spruce, and deciduous species. According to literature, aspen stands usually do not sustain crown fires because fires reaching the crown tend to drop to the ground and burn as surface fire, thereby making them act as natural barriers to fires (Cumming, 2001; DeByle and Winokur, 1985; Jones and DeByle, 1985). Trembling aspen, balsam poplar, and white birch, the most common deciduous stands in boreal forest stands of northern Alberta, have physiological and morphological characteristics (e.g.: high crown base height, high leaf and stem moisture content, smooth bark) that make them ineffective in spreading wildfires (Alberta Government, 2012). Therefore, forest stands with a higher proportion of deciduous species prior to the fire will sustain less severe burns.

Coniferous species such as spruce and pines, on the other hand, have characteristics that can help spread wildfires with highly flammable configuration (Miquelajauregui et al., 2016). The canopy architecture of conifers with deep crowns with low crown base heights, a large number of twigs and needles in the bulk canopies, high resin, and low foliar moisture contents facilitate crown fires (Johnson and Johnson, 1996; Van Wagner, 1983; Wagner, 1977). Since they occur in high density and accumulate needles on the forest floor, they can also support the spread of fire spatially (Alberta Government, 2012; Thompson et al., 2017). According to Miquelajauregui et al., (2016) the structure of conifer stands also influences the burn severity of boreal stands depending on the diameter class distribution and canopy bulk density of spruce and pine stands. Miquelajauregui et al., (2016) also show that the uneven spruce stands to experience low severity fires, and may act as a biotic feedback mechanism, reducing the mean fire severity. In addition to burn severity, forest composition may also influence post-fire regeneration trajectories, alter post-fire tree fall patterns and decomposition rates and nutrient recycling, and modify carbon stocks and fluxes in boreal forests (Boby et al., 2010; Boulanger et al., 2011; Johnstone et al., 2011; Ryan, 2002). According to Johnstone et al., (2010), spruce-dominated forests are vulnerable to shift in deciduous stands as a result of high severity fires and lead to a cooling effect on local climate with less energy absorption and higher transpiration rates (Cumming, 2001). Therefore, closer observation of burn severity and regeneration of boreal stands is essential to understand and predict the future shifts in fire regimes.

Boreal forests consist of many freshwater reserves and approximately 25% of the boreal forest cover in western Canada is characterized by wetlands (Mery et al., 2010; Tarnocai et al., 2011; Thompson et al., 2017). Several studies have investigated the effect of wetland cover and fuel loading levels in wetlands and have reported negative relationships with wildfire susceptibility and severity (Johnston et al., 2015; Schneider et al., 2016; Thompson et al., 2017; Whitman et al., 2018). According to Thompson et al., (2017), the fuel in wetlands may show site-level differences in fuel moisture, phenology, and access to groundwater and may contribute to burning if profound droughts occur. Johnston et al., (2015) reported that the potential of high-frequency fire in graminoid-dominant wetlands is only possible in about 80 years after a significant fire event. Despite these documented findings, the effect of surface waters on the spread of fire and burn severity is still poorly understood. Our results suggest that regardless of land cover (e.g. wetland or forested), surface waters up to 1 km distance from vegetation can protect and/or ameliorate fire damage. Therefore, surface waters in the boreal region play an important role in controlling the spread of severe fires, especially under the increased frequency of wildfires due to global climate change.

When relating the pre-fire species composition with the burn severity, we did not observe any relationship with the commonly used index, dNBR. However, SBIS captured the relationship with pre-fire species composition as well as the duration of the fire, indicating that the combination of the burned extent and burn severity are important for understanding fire behavior. Furthermore, we obtained a stronger relationship between distance from surface waters and SBIS than for dNBR. This indicates that the burn impact provides a better measure of the importance of surface waters in fire behavior than that of burn severity. We, therefore, recommend using SBIS over dNBR when describing the relationship between burn impact and pre-fire conditions.

5. Conclusion

Changes in fire regimes due to global climate change in the boreal region have both social and ecological ramifications. Understanding pre-fire conditions that lead to severe fires may help us forecast future wildfire trajectories. To make a more generalized understanding of fire regime changes, wildfires need to be investigated over large spatial scales and over longer time spans. We used remote-sensing techniques to study pre-fire conditions on burn severity and burn impact using 21 fire events in four boreal forest regions in northern Alberta. To map the pre-fire distribution of canopy species in the burned areas, we successfully employed remote sensing approaches with multitemporal Landsat images. We created the SBIS by combining dNBR (commonly used index of burn severity) and total burned area of different fire events and used them to understand the relationships between pre-fire conditions and burn impact. Our results, generated with reproducible methods and that have broad applicability, confirm that areas dominated by conifers lead to more severe fires while those occupied by deciduous species can reduce burn severity. These methods could be used to closely study the influence of species composition on burn severity over larger spatial scales and over long time scales. Our study also shows that early-season fires may last longer and burn deciduous stands more than do summer fires, and may thus have a greater impact. We have demonstrated a cost-effective means to map species distribution in remote forested areas that may help forest managers to develop more up-to-date forest maps. We showed the importance of surface waters in the boreal region in reducing or inhibiting the spread of wildfires, regardless of the type of nearby ecosystems or plant communities.

CRediT authorship contribution statement

Prabha Amali Rupasinghe: Conceptualization, Data curation, Methodology, Software, Formal analysis, Validation, Visualization, Investigation, Writing - original draft. **Patricia Chow-Fraser:** Conceptualization, Methodology, Investigation, Project administration, Resources, Supervision, Funding acquisition, Writing - review and editing.

Declaration of Competing Interest

The authors declare that they have no known competing financial interests or personal relationships that could have appeared to influence the work reported in this paper.

Acknowledgments

We would like to thank Dr. Michael Waddington and Dr. Francoise-Nicolas Robinne for sharing their experience on wildfire and for providing valuable references and data sources. We also thank Jordan DeBoer, Yuxin Zang, and Sherry Chen for the assistance with image pre-processing and digitizing.

Funding

The research published in this paper is part of the project titled Boreal Water Futures, which is funded by the Global Water Futures programme of the Canada First Research Excellence Fund.

References

Akther, M.S., Hassan, Q.K., 2011. Remote sensing-based assessment of fire danger conditions over boreal forest. IEEE J Sel. Top. Appl. Earth Observ. Remote Sens. 4 (4), 992–999. https://doi.org/10.1109/JSTARS.2011.2165940.

Alberta Forest service, 1985. Alberta Phase 3 Forest Inventory; An OverView (No. ENR Report No. I/86). Alberta Energy and Natural Resources, Edmonton, Alberta, Canada.

Alberta Government, 2019. West of 4th Meridian - Historical Forest Inventory - Phase 3 Maps - Open Government [WWW Document]. URL https://open.alberta.ca/dataset/gda-dfa530fd-1e9d-4649-a984-fe3560a2fb93 (accessed 8.6.20).

Alberta Government, 2012. How Different Tree Species Impact the Spread of Wildfire. https://www1.agric.gov.ab.ca/$department/deptdocs.nsf/all/formain15744/$FILE/tree-species-impact-wildfire-aug03-2012.pdf (accessed on 12/27/2020).

Alberta Parks, 2018. Information & Facilities - Richardson Wildland Provincial Park | Alberta Parks [WWW Document]. URL https://www.albertaparks.ca/parks/northeast/richardson-wpp/information-facilities/ (accessed 8.5.20).

Alberta Wilderness Association, 2021. Straddling on the border of the Northwest Territories and British Columbia, Bistcho is a remote and serene boreal forest wilderness nestled in the far northwestern corner of Alberta. [WWW Document]. Alberta Wilderness Association. URL https://albertawilderness.ca/issues/wildlands/areas-of-concern/bistcho/ (accessed 8.5.20).

Alberta wildfire, 2020. Spatial Wildfire Data | AAF - Agriculture and Forestry [WWW Document]. URL https://wildfire.alberta.ca/resources/historical-data/spatial-wildfire-data.aspx (accessed 12.24.20).

Alonzo, M., Morton, D.C., Cook, B.D., Andersen, H.-E., Babcock, C., Pattison, R., 2017. Patterns of canopy and surface layer consumption in a boreal forest fire from repeat airborne lidar. Environ. Res. Lett. 12 (6), 065004. https://doi.org/10.1088/1748-9326/aa6ade.

Barrett, K., McGuire, A.D., Hoy, E.E., Kasischke, E.S., 2011. Potential shifts in dominant forest cover in interior Alaska driven by variations in fire severity. Ecol. Appl. 21 (7), 2380–2396. https://doi.org/10.1890/10-0896.1.

Boby, L.A., Schuur, E.A.G., Mack, M.C., Verbyla, D., Johnstone, J.F., 2010. Quantifying fire severity, carbon, and nitrogen emissions in Alaska's boreal forest. Ecol. Appl. 20 (6), 1633–1647.

Bolton, D.K., Coops, N.C., Wulder, M.A., 2015. Characterizing residual structure and forest recovery following high-severity fire in the western boreal of Canada using Landsat time-series and airborne lidar data. Remote Sens. Environ. 163, 48–60.

Botey, A.P., Kulig, J.C., 2014. Family functioning following wildfires: recovering from the 2011 slave lake fires. J. Child Fam. Stud. 23 (8), 1471–1483. https://doi.org/10.1007/s10826-013-9802-6.

Boucher, J., Beaudoin, A., Hébert, C., Guindon, L., Bauce, Éric, 2016. Assessing the potential of the differenced Normalized Burn Ratio (dNBR) for estimating burn severity in eastern Canadian boreal forests. Int. J. Wildland Fire 26 (1), 32–45. https://doi.org/10.1071/WF15122.

Boulanger, Y., Sirois, L., Hébert, C., 2011. Fire severity as a determinant factor of the decomposition rate of fire-killed black spruce in the northern boreal forest. Can. J. For. Res. 41 (2), 370–379.

Bourgeau-Chavez, L.L., Grelik, S.L., Billmire, M., Jenkins, L.K., Kasischke, E.S., Turetsky, M.R., 2020. Assessing boreal peat fire severity and vulnerability of peatlands to early season wildland fire. Front. Forests Global Change 3. https://doi.org/10.3389/ffgc.2020.00020.

Canadian Parks and Wilderness Society Northern Alberta, 2016. Alberta's Caribou: a guide to range planning. Vol. 2: Little Smoky.

Chu, T., Guo, X., 2014. Remote sensing techniques in monitoring post-fire effects and patterns of forest recovery in boreal forest regions: a review. Remote Sensing 6, 470–520. https://doi.org/10.3390/rs6010470.

Chu, T., Guo, X., Takeda, K., 2016. Remote sensing approach to detect post-fire vegetation regrowth in Siberian boreal larch forest. Ecol. Ind. 62, 32–46. https://doi.org/10.1016/j.ecolind.2015.11.026.

Chuvieco, E., Riaño, D., Danson, F.M., Martin, P., 2006. Use of a radiative transfer model to simulate the postfire spectral response to burn severity. J. Geophys. Res. Biogeosci. 111 (G4) https://doi.org/10.1029/2005JG000143.

Cocke, A., Fulé, P., Crouse, J., 2005. Comparison of burn severity assessment using Differenced Normalized Burn Ratio and ground data. Int. J. Wildland Fire 14, 189–198. https://doi.org/10.1071/WF04010.

Cumming, S.G., 2001. Forest type and wildfire in the Alberta boreal mixedwood: what do fires burn? Ecol. Appl. 11, 97–110. https://doi.org/10.1890/1051-0761(2001)011[0097:FTAWIT]2.0.CO;2.

DeByle, N.V., Winokur, R.P., 1985. Aspen: ecology and management in the western United States (No. RM-119). US Department of Agriculture, Forest Service, Rocky Mountain Forest and Range Experiment Station, Fort Collins, Colorado, USA.

Fernández-García, V., Quintano, C., Taboada, A., Marcos, E., Calvo, L., Fernández-Manso, A., 2018. Remote sensing applied to the study of fire regime attributes and their influence on post-fire greenness recovery in pine ecosystems. Remote Sensing 10, 733. https://doi.org/10.3390/rs10050733 https://doi.org/733;.

Flannigan, M., Stocks, B., Turetsky, M., Wotton, M., 2009. Impacts of climate change on fire activity and fire management in the circumboreal forest. Glob. Change Biol. 15, 549–560. https://doi.org/10.1111/j.1365-2486.2008.01660.x.

French, N.H., Kasischke, E.S., Bourgeau-Chavez, L.L., Berry, D., 1995. Mapping the location of wildfires in Alaskan boreal forests using AVHRR imagery. Int. J. Wildland Fire 5 (2), 55–62. https://doi.org/10.1071/WF9950055.

French, N.H.F., Kasischke, E.S., Hall, R.J., Murphy, K.A., Verbyla, D.L., Hoy, E.E., Allen, J.L., 2008. Using Landsat data to assess fire and burn severity in the North American boreal forest region: an overview and summary of results. Int. J. Wildland Fire 17 (4), 443–462. https://doi.org/10.1071/WF08007.

Gauthier, S., Bernier, P., Kuuluvainen, T., Shvidenko, A.Z., Schepaschenko, D.G., 2015. Boreal forest health and global change. Science 349 (6250), 819–822. https://doi.org/10.1126/science:aaa9092.

George, C., Rowland, C., Gerard, F., Balzter, H., 2006. Retrospective mapping of burnt areas in Central Siberia using a modification of the normalised difference water index. Remote Sens. Environ. 104 (3), 346–359.

Hall, R.J., Freeburn, J.T., De Groot, W.J., Pritchard, J.M., Lynham, T.J., Landry, R., 2008. Remote sensing of burn severity: experience from western Canada boreal fires. Int. J. Wildland Fire 17, 476–489. https://doi.org/10.1071/WF08013.

Hammill, K.A., Bradstock, R.A., 2006. Remote sensing of fire severity in the Blue Mountains: influence of vegetation type and inferring fire intensity. Int. J. Wildland Fire 15, 213–226. https://doi.org/10.1071/WF05051.

Johnson, E.A., Miyanishi, K., Bridge, S.R.J., 2001. Wildfire regime in the boreal forest and the idea of suppression and fuel buildup. Conserv. Biol. 15 (6), 1554–1557.

Johnson, E.A., Johnson, E.A., 1996. Fire and vegetation dynamics: studies from the North American boreal forest. Cambridge University Press, Cambridge, United Kingdom.

Johnston, D.C., Turetsky, M.R., Benscoter, B.W., Wotton, B.M., 2015. Fuel load, structure, and potential fire behaviour in black spruce bogs. Can. J. For. Res. 45 (7), 888–899. https://doi.org/10.1139/cjfr-2014-0334.

Johnstone, J.F., Hollingsworth, T.N., Chapin III, F.S., Mack, M.C., 2010. Changes in fire regime break the legacy lock on successional trajectories in Alaskan boreal forest. Glob. Change Biol. 16 (4), 1281–1295.

Johnstone, J.F., Rupp, T.S., Olson, M., Verbyla, D., 2011. Modeling impacts of fire severity on successional trajectories and future fire behavior in Alaskan boreal forests. Landscape Ecol. 26 (4), 487–500.

Jones, J.R., DeByle, N.V., 1985. Genetics and variation in Aspen: Ecology and Management in the Western United States (Technical report No. RM-119). USDA Forest Service, Rocky Mountain Forest and Range Experiment Station, Fort Collins, CO.

Karna, Y.K., Penman, T.D., Aponte, C., Bennett, L.T., 2019. Assessing legacy effects of wildfires on the crown structure of fire-tolerant eucalypt trees using airborne lidar data. Remote Sensing 11 (20), 2433. https://doi.org/10.3390/rs11202433.

Kasischke, E.S., Christensen Jr, N.L., Stocks, B.J., 1995. Fire, global warming, and the carbon balance of boreal forests. Ecol. Appl. 5, 437–451. https://doi.org/10.2307/1942034.

Kasischke, E.S., French, N.H.F., 1995. Locating and estimating the areal extent of wildfires in Alaskan boreal forests using multiple-season AVHRR NDVI composite data. Remote Sens. Environ. 51 (2), 263–275.

Kasischke, E.S., Tanase, M.A., Bourgeau-Chavez, L.L., Borr, M., 2011. Soil moisture limitations on monitoring boreal forest regrowth using spaceborne L-band SAR data. Remote Sens. Environ. 115 (1), 227–232.

Keeley, J., 2009. Fire intensity, fire severity and burn severity: A brief review and suggested usage. Int. J. Wildland Fire 18, 116–126. https://doi.org/10.1071/WF07049.

Kelhä, V., Rauste, Y., Häme, T., Sephton, T., Buongiorno, A., Frauenberger, O., Soini, K., VenäLäinen, A., Miguel-Ayanz, J.S., Vainio, T., 2003. Combining AVHRR and ATSR satellite sensor data for operational boreal forest fire detection. Int. J. Remote Sens. 24 (8), 1691–1708.

Key, C.H., Benson, N.C., 2005. Landscape assessment: ground measure of severity, the Composite Burn Index; and remote sensing of severity, the Normalized Burn Ratio. FIREMON: Fire effects monitoring and inventory system 2004.

Knapp, E.E., Keeley, J.E., Ballenger, E.A., Brennan, T.J., 2005. Fuel reduction and coarse woody debris dynamics with early season and late season prescribed fire in a Sierra Nevada mixed conifer forest. For. Ecol. Manage. 208 (1-3), 383–397.

Knapp, E.E., Schwilk, D.W., Kane, J.M., Keeley, J.E., 2007. Role of burning season on initial understory vegetation response to prescribed fire in a mixed conifer forest. Can. J. For. Res. 37 (1), 11–22. https://doi.org/10.1139/x06-200.

Kokaly, R.F., Rockwell, B.W., Haire, S.L., King, T.V.V., 2007. Characterization of post-fire surface cover, soils, and burn severity at the Cerro Grande Fire, New Mexico, using hyperspectral and multispectral remote sensing. Remote Sens. Environ. 106 (3), 305–325. https://doi.org/10.1016/j.rse.2006.08.006.

Krawchuk, M.A., Haire, S.L., Coop, J., Parisien, M.A., Whitman, E., Chong, G., Miller, C., 2016. Topographic and fire weather controls of fire refugia in forested ecosystems of northwestern North America. Ecosphere 7, 1–18. https://doi.org/10.1002/ecs2.1632.

Lentile, L.B., Holden, Z.A., Smith, A.M., Falkowski, M.J., Hudak, A.T., Morgan, P., Lewis, S.A., Gessler, P.E., Benson, N.C., 2006. Remote sensing techniques to assess active fire characteristics and post-fire effects. Int. J. Wildland Fire 15, 319–345. https://doi.org/10.1071/WF05097.

Leon, J.R.R., Van Leeuwen, W.J., Casady, G.M., 2012. Using MODIS-NDVI for the modeling of post-wildfire vegetation response as a function of environmental conditions and pre-fire restoration treatments. Remote Sensing 4, 598–621. https://doi.org/10.3390/rs4030598.

Liu, Q.J., Takamura, T., Takeuchi, N., Shao, G., 2002. Mapping of boreal vegetation of a temperate mountain in China by multitemporal Landsat TM imagery. Int. J. Remote Sens. 23 (17), 3385–3405. https://doi.org/10.1080/01431160110076171.

Loboda, T., O'Neal, K.J., Csiszar, I., 2007. Regionally adaptable dNBR-based algorithm for burned area mapping from MODIS data. Remote Sens. Environ. 109 (4), 429–442. https://doi.org/10.1016/j.rse.2007.01.017.

Lucas, R., Clewley, D., Rosenqvist, A., Kellndorfer, J., Walker, W., Hoekman, D., Shimada, M., de Mesquita Jr, H.N., 2012. Global forest monitoring with synthetic aperture radar (SAR) data. Earth Observ. Global Changes 273.

Lydersen, J.M., Collins, B.M., Brooks, M.L., Matchett, J.R., Shive, K.L., Povak, N.A., Kane, V.R., Smith, D.F., 2017. Evidence of fuels management and fire weather influencing fire severity in an extreme fire event. Ecol. Appl. 27 (7), 2013–2030. https://doi.org/10.1002/eap.1586.

Matsuura, Y., 2010. Soil carbon and nitrogen storage in Siberian permafrost region/A. Osawa, OA Zyryanova, Y. Matsuura, T. Kajimoto, RW Wein. Permafrost Ecosystems: Siberian Larch Forests. Ecol. Stud. 209, 149–163.

Mery, G., Katila, P., Galloway, G., Alfaro, R.I., Kanninen, M., Lobovikov, M., Varjo, J., 2010. Forests and society-responding to global drivers of change, IUFRO World Series. International Union of Forest Research Organizations (IUFRO), Vantaa, Finland.

Miller, J.D., Thode, A.E., 2007. Quantifying burn severity in a heterogeneous landscape with a relative version of the delta Normalized Burn Ratio (dNBR). Remote Sens. Environ. 109 (1), 66–80. https://doi.org/10.1016/j.rse.2006.12.006.

Miller, J.D., Yool, S.R., 2002. Mapping forest post-fire canopy consumption in several overstory types using multi-temporal Landsat TM and ETM data. Remote Sens. Environ. 82 (2-3), 481–496. https://doi.org/10.1016/S0034-4257(02)00071-8.

Miquelajauregui, Y., Cumming, S.G., Gauthier, S., Chen, H.Y.H., 2016. Modelling variable fire severity in boreal forests: effects of fire intensity and stand structure. PLoS ONE 11 (2), e0150073. https://doi.org/10.1371/journal.pone.0150073.

Moreno Ruiz, J.A., Riaño, D., Arbelo, M., French, N.H.F., Ustin, S.L., Whiting, M.L., 2012. Burned area mapping time series in Canada (1984–1999) from NOAA-AVHRR LTDR: a comparison with other remote sensing products and fire perimeters. Remote Sens. Environ. 117, 407–414.

Murphy, K., Reynolds, J., Koltun, J., 2008. Evaluating the ability of the differenced Normalized Burn Ratio (dNBR) to predict ecologically significant burn severity in Alaskan boreal forests. Int. J. Wildland Fire 17, 490–499. https://doi.org/10.1071/WF08050.

Natural Resources Canada, 2017. Canadian Wildland Fire Information System | CWFIS Datamart [WWW Document]. URL https://cwfis.cfs.nrcan.gc.ca/datamart (accessed 8.6.20).

Ononye, A., Vodacek, A., Saber, E., 2007. Automated extraction of fire line parameters from multispectral infrared images. Remote Sens. Environ. 108 (2), 179–188. https://doi.org/10.1016/j.rse.2006.09.029.

Pan, Y., Birdsey, R.A., Fang, J., Houghton, R., Kauppi, P.E., Kurz, W.A., Phillips, O.L., Shvidenko, A., Lewis, S.L., Canadell, J.G., Ciais, P., Jackson, R.B., Pacala, S.W., McGuire, A.D., Piao, S., Rautiainen, A., Sitch, S., Hayes, D., 2011. A large and persistent carbon sink in the world's forests. Science 333 (6045), 988–993.

Parisien, M.-A., Kafka, V., Hirsch, K., Todd, J., Lavoie, S., Maczek, P., 2005. Mapping Wildfire Susceptibility with the BURN-P3 Simulation Model (No. NOR-X-405). Natural Resources Canada, Canadian Forest Service, Northern Forestry Centre.

Parks, S.A., Dillon, G.K., Miller, C., 2014. A new metric for quantifying burn severity: the relativized burn ratio. Remote Sensing 6, 1827–1844. https://doi.org/10.3390/rs6031827.

Peddle, D.R., Hall, R.J., Jackson, C.D., Soenen, S.A., Gibb, M.R., Juhlin, D.T., 2007. MFM Canopy Reflectance Modeling and Normalized Burn Ratio Assessment of Pre-fire Overstory Canopy Structure and Post-Fire Burn Severity at the Lost Creek Fire, Alberta Rocky Mountains 12.

Potapov, P., Hansen, M.C., Stehman, S.V., Loveland, T.R., Pittman, K., 2008. Combining MODIS and Landsat imagery to estimate and map boreal forest cover loss. Remote Sens. Environ. 112 (9), 3708–3719.

Remmel, T.K., Perera, A.H., 2001. Fire mapping in a northern boreal forest: assessing AVHRR/NDVI methods of change detection. For. Ecol. Manage. 152 (1-3), 119–129.

Robinne, F.-N., Parisien, M.-A., Flannigan, M., 2016. Anthropogenic influence on wildfire activity in Alberta, Canada. Int. J. Wildland Fire 25, 1131–1143. https://doi.org/10.1071/WF16058.

Ryan, K.C., 2002. Dynamic interactions between forest structure and fire behavior in boreal ecosystems. Silva Fennica 36, 13–39.

San-Miguel, I., Andison, D.W., Coops, N.C., Rickbeil, G.J.M., 2016. Predicting post-fire canopy mortality in the boreal forest from dNBR derived from time series of Landsat data. Int. J. Wildland Fire 25 (7), 762–774. https://doi.org/10.1071/WF15226.

Schneider, R.R., Devito, K., Kettridge, N., Bayne, E., 2016. Moving beyond bioclimatic envelope models: integrating upland forest and peatland processes to predict ecosystem transitions under climate change in the western Canadian boreal plain. Ecohydrology 9 (6), 899–908. https://doi.org/10.1002/eco.v9.610.1002/eco.1707.

Schoennagel, T., Veblen, T.T., Romme, W.H., 2004. The interaction of fire, fuels, and climate across Rocky Mountain forests. Bioscience 54, 661–676. https://doi.org/10.1641/0006-3568(2004)054[0661:TIOFFA]2.0.CO;2.

Schroeder, T.A., Wulder, M.A., Healey, S.P., Moisen, G.G., 2011. Mapping wildfire and clearcut harvest disturbances in boreal forests with Landsat time series data. Remote Sens. Environ. 115 (6), 1421–1433.

Shorohova, E., Kneeshaw, D., Kuuluvainen, T., Gauthier, S., 2011. Variability and dynamics of old-growth forests in the circumbolear zone: implications for conservation, restoration and management. Silva Fenn 45, 785–806. https://doi.org/10.14214/sf.72.

Soverel, N., Coops, N., Perrakis, D., Daniels, L., Gergel, S., 2011. The transferability of a dNBR-derived model to predict burn severity across 10 wildland fires in western Canada. Int. J. Wildland Fire 20, 518–531. https://doi.org/10.1071/WF10081.

Soverel, N.O., Perrakis, D.D.B., Coops, N.C., 2010. Estimating burn severity from Landsat dNBR and RdNBR indices across western Canada. Remote Sens. Environ. 114 (9), 1896–1909. https://doi.org/10.1016/j.rse.2010.03.013.

Steffen, W., Richardson, K., Rockstrom, J., Cornell, S.E., Fetzer, I., Bennett, E.M., Biggs, R., Carpenter, S.R., de Vries, W., de Wit, C.A., Folke, C., Gerten, D., Heinke, J., Mace, G.M., Persson, L.M., Ramanathan, V., Reyers, B., Sorlin, S., 2015. Planetary boundaries: guiding human development on a changing planet. Science 347 (6223), 1259855. https://doi.org/10.1126/science:1259855.

Stralberg, D., Wang, X., Parisien, M.-A., Robinne, F.-N., Sólymos, Péter, Mahon, C.L., Nielsen, S.E., Bayne, E.M., 2018. Wildfire-mediated vegetation change in boreal forests of Alberta, Canada. Ecosphere 9 (3), e02156. https://doi.org/10.1002/ecs2.2156.

Tarnocai, C., Kettles, I.M., Lacelle, B., 2011. Peatlands of Canada; Geological Survey of Canada, Open File 6561; map. Natural Resources of Canada/Ressources naturelles Canada.

Thompson, D.K., Parisien, M.-A., Morin, J., Millard, K., Larsen, C.P.S., Simpson, B.N., 2017. Fuel accumulation in a high-frequency boreal wildfire regime: from wetland to upland. Can. J. For. Res. 47 (7), 957–964. https://doi.org/10.1139/cjfr-2016-0475.

Thompson, M.P., Calkin, D.E., 2011. Uncertainty and risk in wildland fire management: a review. J. Environ. Manage. 92 (8), 1895–1909. https://doi.org/10.1016/j.jenvman.2011.03.015.

Tymstra, C., Wang, D., Rogeau, M.-P., 2005. Alberta wildfire regime analysis (Wildfire Science and Technology Report No. PFFC-01-5). Alberta Department of Sustainable Resource Development, Forest Protection Division, Edmonton AB.

UNESCO World Heritage Center, 2020. Wood Buffalo National Park [WWW Document]. UNESCO World Heritage Centre. URL https://whc.unesco.org/en/list/256/ (accessed 8.5.20).

U.S. Fire Administration, 2005. The Seasonal Nature of Fires. Department of Homeland Security Federal Emergency Management Agency United States Fire Administration National Fire Data Center, https://www.usfa.fema.gov/downloads/pdf/publications/fa-236.pdf (Accessed on 05/07/2021).

USGS, 2016a. Landsat Missions; Landsat 5 [WWW Document]. Fact Sheet. URL https://www.usgs.gov/core-science-systems/nli/landsat/landsat-5?qt-science_support_page_related_con=0#qt-science_support_page_related_con (accessed 8.5.20).

USGS, 2016b. Landsat Missions; Landsat 7 [WWW Document]. Fact Sheet. URL https://www.usgs.gov/core-science-systems/nli/landsat/landsat-7?qt-science_support_page_related_con=0#qt-science_support_page_related_con (accessed 8.5.20).

Van Wagner, C.E., 1983. Fire behavior in northern conifer forests and shrublands. In: Wein, R.W., MacLean, D. (Eds.), The role of fire in northern circumpolar ecosystems. John Wiley & Sons Inc, Chichester, England.

Wagner, C.E.V., 1977. Conditions for the start and spread of crown fire. Can. J. For. Res. 7 (1), 23–34. https://doi.org/10.1139/x77-004.

Whitman, E., Parisien, M.-A., Holsinger, L.M., Park, J., Parks, S.A., 2020. A method for creating a burn severity atlas: an example from Alberta, Canada. Int. J. Wildland Fire 29 (11), 995–1008. https://doi.org/10.1071/WF19177.

Whitman, E., Parisien, M.-A., Thompson, D.K., Hall, R.J., Skakun, R.S., Flannigan, M.D., 2018. Variability and drivers of burn severity in the northwestern Canadian boreal forest. Ecosphere 9 (2), e02128. https://doi.org/10.1002/ecs2.2128.

Wulder, M.A., White, J.C., Alvarez, F., Han, T., Rogan, J., Hawkes, B., 2009. Characterizing boreal forest wildfire with multi-temporal Landsat and LIDAR data. Remote Sens. Environ. 113 (7), 1540–1555.